Source: **Motorola**
Title: **Model Components and Results for Spatial Channel Model**
Document for: **Discussion**

1. SUMMARY

This contribution presents a number of items related to the generation of the Spatial Channel Model parameters. This includes: a description of the various components of the Motorola proposal given in recent contributions, including statistical results from the channel model for a test environment. The following details are described:

- Description of the steps involved in generating a Spatial channel model from [1] and the corresponding output statistics of key parameters
- Additional Models
    - Adding Randomness to describe the behavior of measured data, e.g. PDP & PAS
    - Adding Polarization to the basic model, covered in SCM-049.

2. CORRELATED SPATIAL CHANNEL MODEL DESCRIPTION

The procedure for generating a correlated spatial channel model is described by the following steps, for a given environment type. Channel model parameters and distributions are defined based on various measurements which have been presented in the literature to achieve accurate spatial and temporal behaviors.

Step 1: Select correlated log normal random variables DS:AS:SF from predefined distributions

Based on measurements and analysis described in [2][3][4], the parameters for azimuth spread (AS), delay spread (DS), and log normal shadow fading (LN), are shown to be significantly correlated. Each of these parameters is shown to obey a log-normal distribution, and correlated by the coefficient ρ. Figure 1 illustrates an example of a log-normal fit to a distribution of measured delay spread. The following values are given from [5].

$\rho_{\alpha\beta}$ = Correlation between DS & AS = +0.5
$\rho_{\gamma\beta}$ = Correlation between LN & AS = -0.75
$\rho_{\gamma\alpha}$ = Correlation between LN & DS = -0.75

The random variables for correlating DS, AS, and LN shadowing are generated using equation 1, where n refers to the nth base station (BS). α, β, and γ are the correlated zero-mean unit variance Gaussian distributed random variables associated with the DS, AS, and LN, respectively, and w_{n1}, w_{n2}, and w_{n3} are unit-variance, independent Gaussian noise samples.

$$\begin{bmatrix} \alpha_n \\ \beta_n \\ \gamma_n \end{bmatrix} = \begin{bmatrix} \rho_{\alpha\alpha} & \rho_{\alpha\beta} & \rho_{\alpha\gamma} \\ \rho_{\beta\alpha} & \rho_{\beta\beta} & \rho_{\beta\gamma} \\ \rho_{\gamma\alpha} & \rho_{\gamma\beta} & \rho_{\gamma\gamma} \end{bmatrix}^{1/2} \begin{bmatrix} w_{n1} \\ w_{n2} \\ w_{n3} \end{bmatrix}, \qquad (1)$$

The LN shadow fading component is typically correlated between Base Stations (BS). A method to produce this is shown in [6].

The cumulative distribution functions of DS, LN, and AS are described in terms of the correlated Gaussian random variables that characterize their distributions [2][3][4]. Using nomenclature from[4] the distribution of DS, AS, and LN are given by:

$\sigma_{Dn} = 10\wedge(\varepsilon_D\alpha_{n\,+}\,\mu_D)$, $\mu_D = E\{\log10(\sigma_{DS})\}$ $\mathrm{Std}\{\log10(\sigma_{DS})\}$ (4)

$\sigma_{An} = 10\wedge(\varepsilon_A\beta_{n\,+}\,\mu_A)$, $\mu_D = E\{\log10(\sigma_{DS})\}$ $\mathrm{Std}\{\log10(\sigma_{DS})\}$ (5)

$\sigma_{LN} = \sigma_{SF}\gamma_n$ (dB) (6)

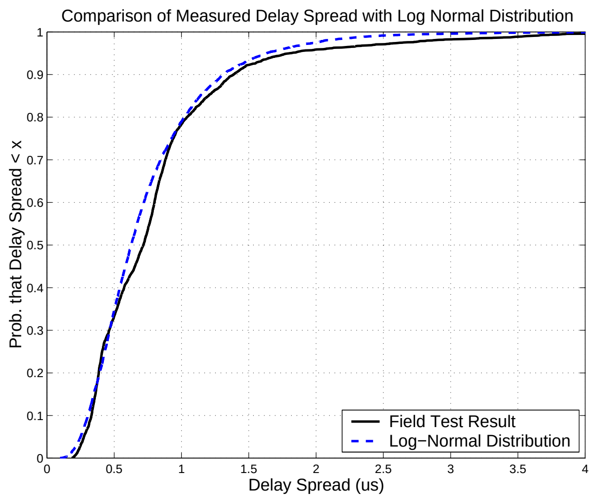

Figure 1, Example of Delay Spread fit to a Log Normal Distribution

Step 2: Select BS σ_{AoD} = r * AS, and draw 6 AoAs

The relationship between the Gaussian σ_{AoD} and the Laplacian σ_{PAS} describes the nature of the spatial distribution of power versus angle. As discussed in [7], the sigmas of the non-power-weighted and power-weighted functions are proportional such that: $\sigma_{AoD} / \sigma_{PAS} = r$.

Step 3: Select 6 log normally distributed random powers, typical σ = 3dB. (set σ = 0 if no randomness is desired in ray powers)

Use of randomizing noise will be discussed in a later section.

Step 4: Apply a power scaling envelope (exponential function of σ_{AoD} and σ_{PAS}) to the ray powers and normalize to unity power to generate a Laplacian PAS

Equation 7 defines the expected power $E(|\alpha|^2)$ for a given angle ϕ.

$$E\left\{|\alpha|^2 \mid \phi\right\} \propto \exp\left(\frac{\phi^2}{2\left(\sigma_{AoD}^2\right)} - \sqrt{2}\frac{|\phi|}{\sigma_{PAS}}\right) \quad (7)$$

where $P_A(\phi)$ is the Laplacian power azimuth spectrum characterized by σ_{PAS}, and $f_A(\phi)$ is the Gaussian AoD distribution characterized by $\sigma_{AoD.}$ The envelope is truncated as described in [7], not show in the plot.

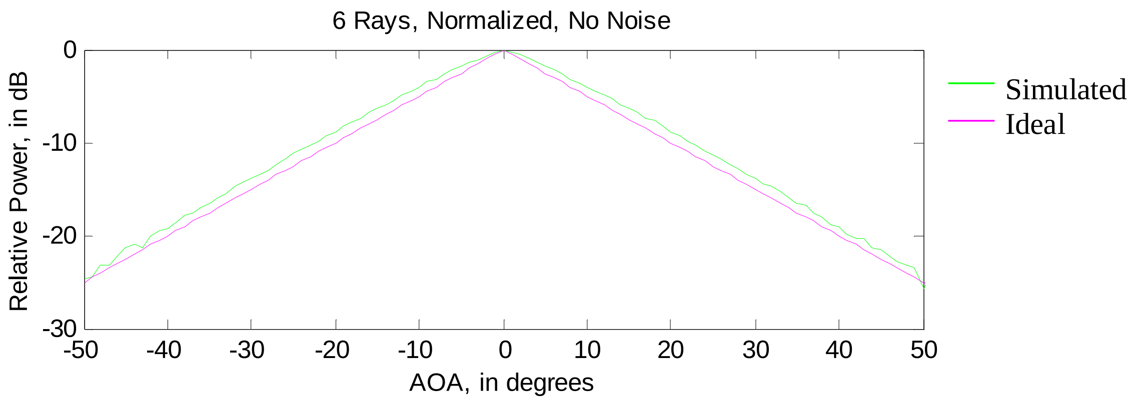

Figure 2, Average PAS after multiplying by Envelope Equation

As shown in Figure 2, when 6 Rays are normalized to unity power, there is a slight change to the envelope, but this doesn't significantly change the Laplacian shape of the PAS.

Step 5: Generate N excess delays for each of the rays from an exponential distribution, assign previously defined ray-powers to each delay, and scale delays to achieve target delay spread.

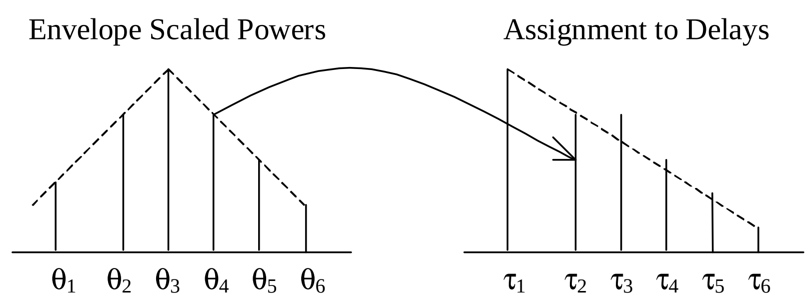

Figure 3, Simulated Power Delay Profile, 6 ray example

The powers obtained above are mapped to delays as shown in Figure 3. Optionally, some re-ordering may be done in the assignment of powers to delays. The sorted exponential delays assigned to the individual rays are scaled to achieve the desired delay spread value by first dividing each ray delay value by the current rms delay spread value and then multiplying by the desired rms delay spread value.

Step 6: Choose 20 sub-rays at the BS to replace each ray to produce 2^o angle spread

A technique described in [8] is shown in Figure 4 as a method to spread sub-rays to produce a Laplacian PAS distribution. This technique has the advantage that all rays are of equal power so the fading behavior converges quickly with a good match to Rayleigh statistics. The result for a 2^o angle spread is shown in Figure 5.

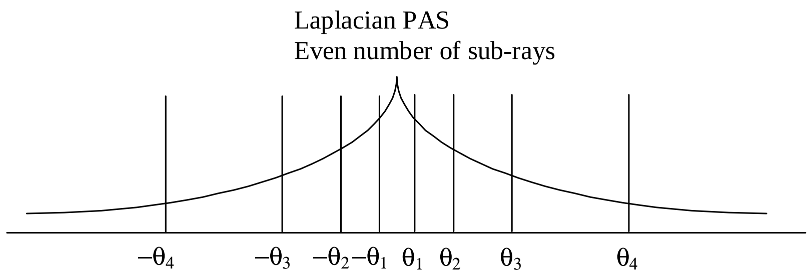

Figure 4, Example method for distribution of Sub-rays in angle based on Laplacian PAS

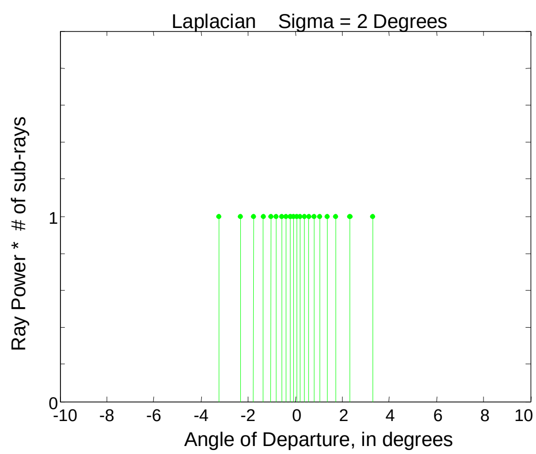

Figure 5, Example of 20 equal power sub-rays to generate a Laplacian spread per ray at the BS

Step 7: Choose N AoAs at the MS based on a given model with composite AS = 70^o, or an urban canyon assumption

A model [9] for MS AoA is developed from measured data is shown in Figure 6 and has an average value of composite AS = 70^o. This model describes the statistical behavior of ray arrivals and is described by a exponential function that is dependent on the fraction of the total power in each arriving ray. The model shows that the higher the fraction of power in a ray, the more likely it is to arrive in the LOS direction to the BS. Weaker rays arrive more uniformly.

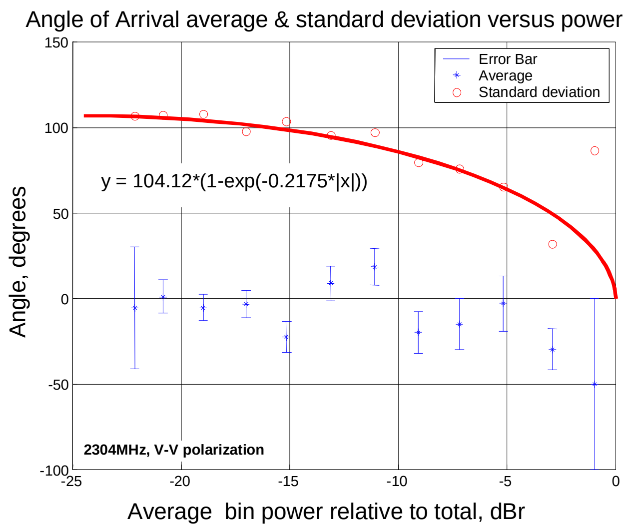

Figure 6, AoA statistics at the MS

Step 8: Choose 20 sub-rays at the MS to replace each ray to produce 35^o angle spread

Careful measurements described in [10] indicate that the per-path AS at the MS can be described by a Cauchy distribution. Assuming a Laplacian distribution with a fixed value of σ = 35^o can be considered a good approximation. This also matches results obtained from other techniques[11].

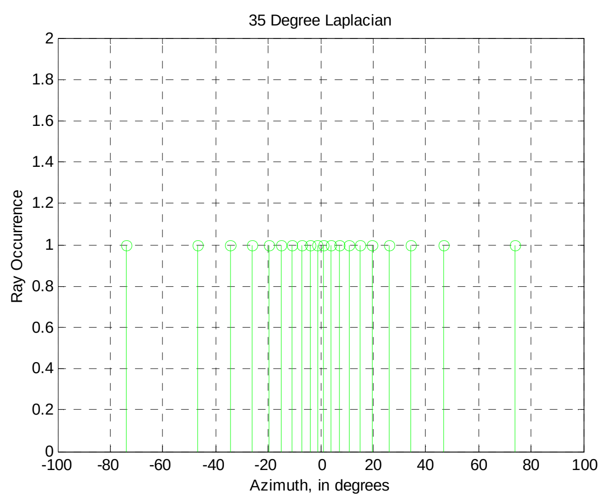

Figure 7, Distribution of 20 equal power sub-rays to generate a Laplacian spread per ray at the MS

Each of the 6 rays are composed of 20 sub-rays in order to define the proper spread. The sub-rays are of equal constant amplitudes and uniformly distributed starting phases between [0,2*pi]. The angle of the sub-ray at the MS is chosen from a Laplacian distribution with a standard deviation of 35 degrees[10][11] and a mean equal to the ray AoA. This is illustrated in Figure 7. The power of each sub-ray is assigned 1/20th the power of each ray in step 1. The excess delay and average AoA is also inherited from each ray.

Step 9: Scale sub-ray components by the appropriate antenna gain based on its AOA or AOD

The power in the channel was normalized to unity in previous steps, which is consistent with an omni antenna gain assumption. For pattern shapes, each sub-ray is adjusted by the antenna gain as shown in Figure 8.

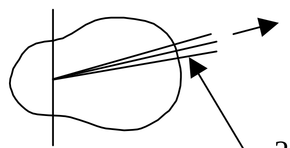

Figure 8, Scaling Sub-rays by Antenna Gain Pattern

3. STATISTICAL RESULTS OF THE SPATIAL CHANNEL MODEL

The following plots result from running the channel model for a number of drops, and gathering statistics on a relevant parameters.

Since the parameters are still to be defined, the environment assumptions for these experiments were taken from[4]:

Shadow fading	7.9 dB
$E\{\sigma_A\}$	13^o
μ_A	0.95
ε_A	0.44
$E\{\sigma_D\}$	1.2 μS
μ_D	-6.08
ε_D	0.35

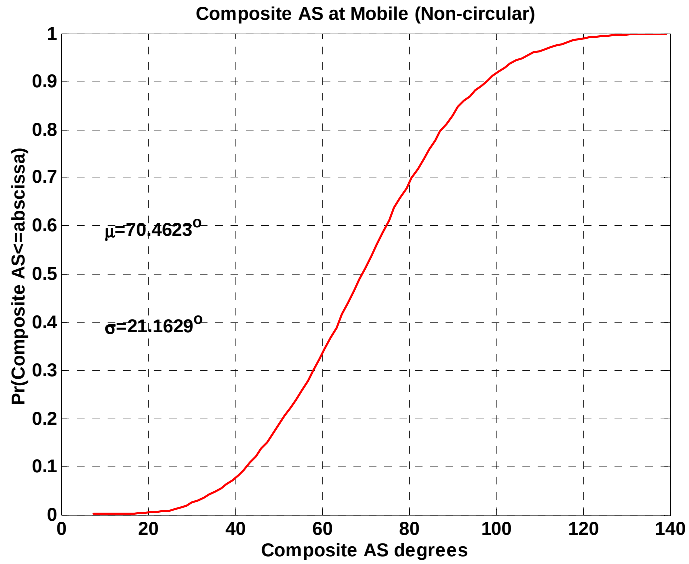

Figure 9, Simulated Composite AS at UE

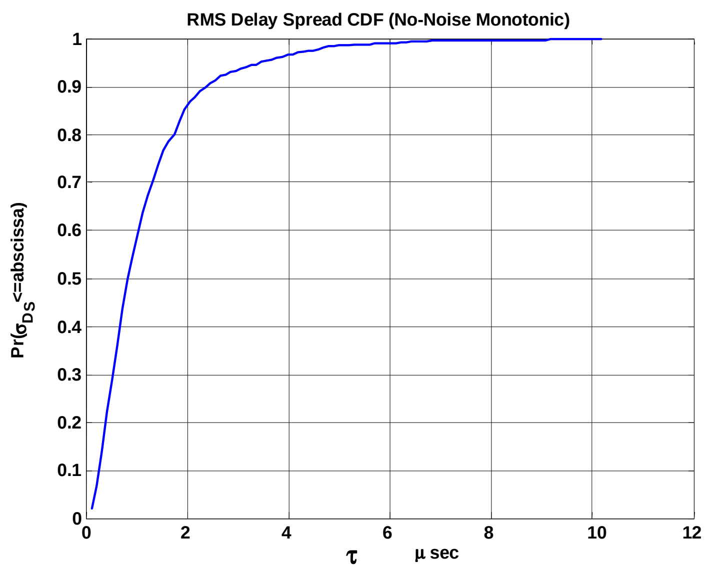

Figure 10, Simulated RMS delay Spread

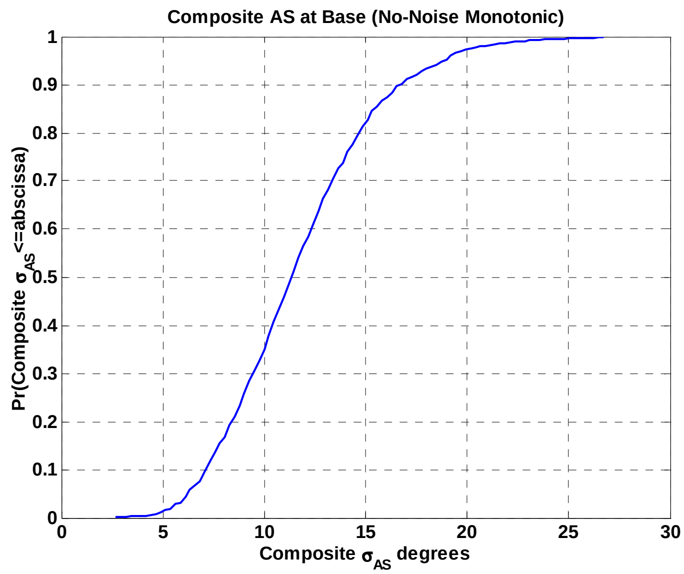

Figure 11, Simulated Composite AS at base

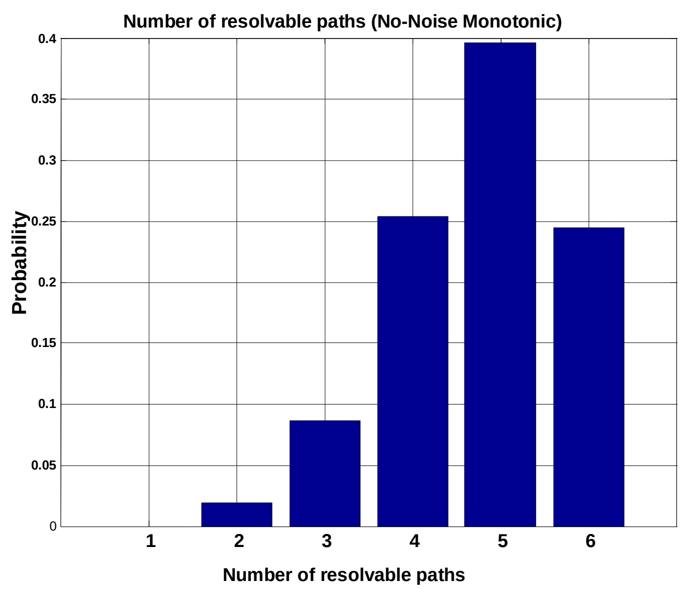

Figure 12, Number of Resolvable Paths for Simulated Reference Channel

3.1 Additional Model Components

3.1.1 Common Reflector

[6] describes a method to define and evaluate the effect of a common reflector using the same technique which defines each of the standard 6 rays. The geometric assumptions of the common reflector will define the AoD, and AoAs for each MS.

In a spatial channel model, it is important to describe the spatial behavior of the path between the BS and the MS. In some cases, a reflector that contributes to the composite signal of a MS is common to the paths of other MSs. This effects the multiple antenna performance because paths to different MSs cannot be separated in angle.

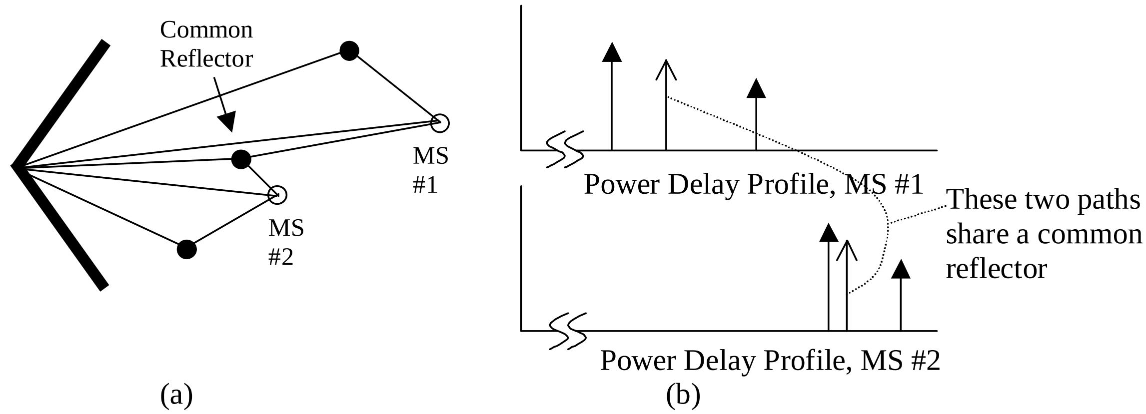

Figure 13, Common Reflector Example Diagram (a), and Power Delay Profile Illustration (b)

Figure 13a illustrates an example of two MSs in a sector, each experiencing a multipath channel to the BS where one component of the multipath shown in Figure 13a&b is common. The angle of departure (AoD) is illustrated in Figure 14 where the common reflector is shown by the signal at about –2 degrees.

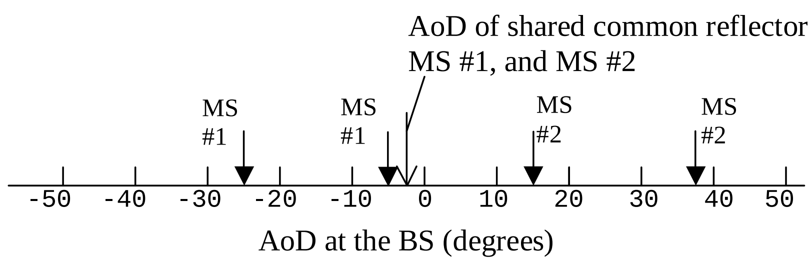

Figure 14, Angle of Departure at BS illustrating common reflector

When a common reflector is desired, it will be chosen after selection of the BS locations, and prior to selecting other channel components. Path delays, and angles are calculated geometrically for all components that are associated with the common reflector. These path components are held constant during the drop, while other components, such as the path amplitude or non-common path parameters may be scaled during the procedure described below. For example, DS or AS may be scaled but the angles and delays associated with the common reflector are held constant to preserve the relationship required by the common reflector.

3.1.2 Use of Randomized Ray Powers & Delays

Since measured data has some amount of randomness evident in both the PAS and the Power Delay Profile, a method for adding randomness is shown. Measurements [12] support the observation of a trend of decreasing power with increasing delay where some amount of randomness is seen in powers and delays. In order to reproduce this effect in the channel model, a method of adding randomness to the average ray powers, affecting both the PAS and PDP is shown.

In the channel model presented above, a log-normal random noise value can be assigned to the 6 Rays in Step 3. This randomness will then be scaled by the exponential envelope of the PAS, and normalized per drop in Step 4, to result in the average over many drops being Laplacian. Figure 15 illustrates a single drop where both a no-noise and a noise case is illustrated. When assigning powers to delays, decreasing powers are assigned to increasing delays. Figure 16 illustrates the no-noise and noise cases which have been applied to exponential delays. When noise is added to the powers as described, the delay assignment is made with the pre-randomized powers, and the result using the randomized power will thus introduce the randomness into the PDP while preserving the trend of decreasing power with time.

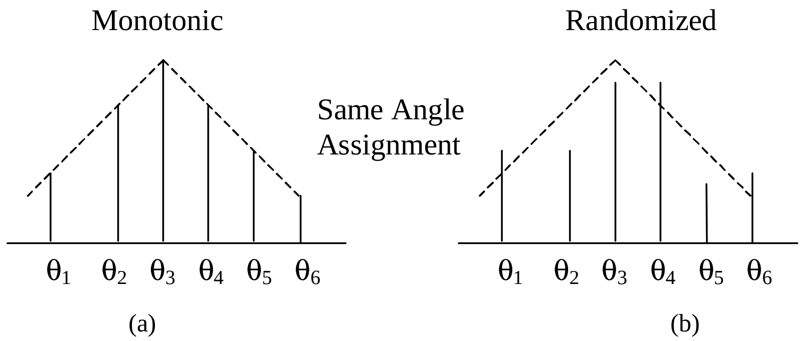

Figure 15, Illustration of Randomizing the Average Powers for a Channel Instance

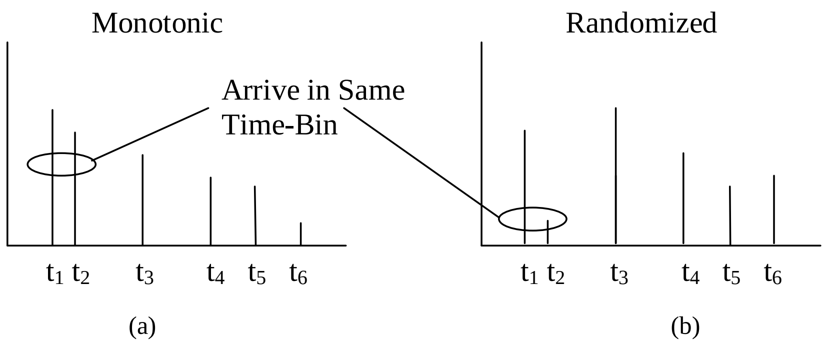

Figure 16, Illustration of Applying Powers to Delays, where t_1 & t_2 fall in the same time bin

Measurements reported in [13] illustrate the randomness experienced in the power delay profile. Significant variations are seen from drop to drop, and this produces the effect of having a mix of strong and weak ray powers arriving in the same time bin, as shown in Figure 16 b. This effect is not present in the monotonic (no-noise) technique. Optionally, re-ordering of the assignments of powers to delays may be done to produce different randomizing effects. One method was described in [6].

Figure 17a illustrates the uniform initial powers used in generating the channel model prior to applying the envelope. In this case, applying the envelope produces a monotonic average PAS. With randomness added as shown in Figure 17b, the per drop result will vary, which is more in line with what is observed in measurements. The red data points in Figure 17b illustrate the randomized powers for a single drop. The blue data points represent several drops.

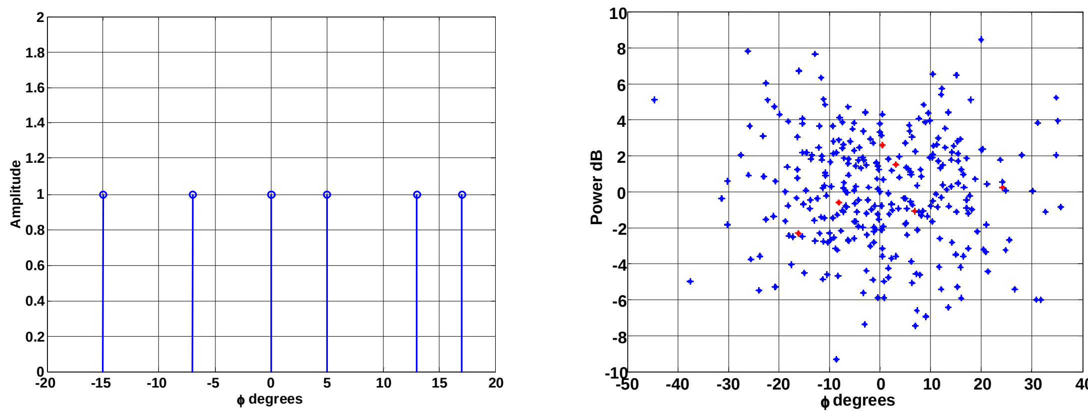

(a) σ = 0dB noise (b) σ = 3dB log normal noise

Figure 17, Selecting initial Ray Powers prior to applying Envelope

Figure 18 illustrates the use of the log-normal randomizing noise to modify the ray powers. The blue data points show the result of the applying the envelope equation to a number of channel instances of 6 ray powers. Each group of 6 is normalized to unity power. The average PAS is also shown. The presence of randomizing noise does not change the envelope or the calculated Average PAS.

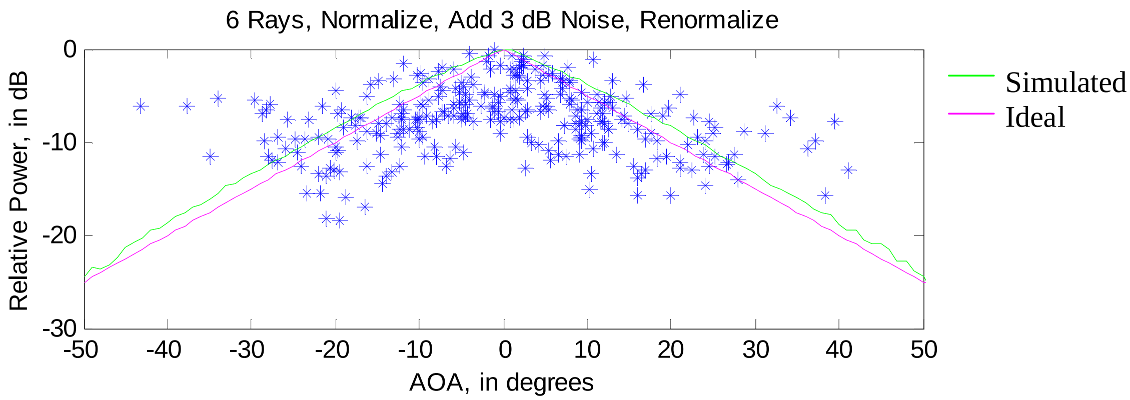

Figure 18, PAS from groups of 6 rays, 3dB log normal starting powers, normalized to unity

4. CONCLUSION

In this contribution, a multi-step process was illustrated as a technique to generate the spatio-temporal channel. The process is easily implemented, and has a minimum of parameters.

A description of a correlated spatial channel model is given with examples of the resulting distributions obtained.

A randomizing noise was shown which reproduces the variation in average power seen in measured data. This noise is applied before multiplying by an exponential envelope to modify the average power in each ray. It produces random variations typically seen in both AS and DS.

5. REFERENCES

[1] Motorola, "Correlated Spatial Channel Model", SCM-029, Conference Call, June 4th 2002.
[2] L. Greenstein, V. Erceg, Y. S. Yeh, M. V. Clark, "A New Path-Gain/Delay-Spread Propagation Model for Digital Cellular Channels," IEEE Transactions on Vehicular Technology, VOL. 46, NO.2, May 1997, pp.477-485.
[3] E. Sousa, V. Jovanovic, C. Daigneault, "Delay Spread Measurements for the Digital Cellular Channel in Toronto," IEEE Transactions on Vehicular Technology, VOL. 43, NO.4, Nov 1994, pp.837-847.
[4] A. Algans, K. I. Pedersen, P. Mogensen, "Experimental Analysis of the Joint Statistical Properties of Azimuth Spread, Delay Spread, and Shadow Fading," IEEE Journal on Selected Areas in Communications, Vol. 20, No. 3, April 2002, pp. 523-531.
[5] L. M. Correia, Wireless Flexible Personalized Communications, COST 259: European Co-operation in Mobile Radio Research, Chichester: John Wiley & Sons, 2001.
[6] Motorola, "Correlated Spatial Channel Model", SCM-020, Conference Call, May 3rd, 2002.
[7] K. Pedersen, P. Morgensen, B. Fleury, "A Stochastic Model of the Temporal and Azimuthal Dispersion Seen at the Base Station in Outdoor Propagation Environments," IEEE Transactions on Vehicular Technology, VOL. 49, NO.2, March 2000, pp.437-447.
[8] Motorola, "Spatial Channel Model Issues", SCM-033r1, Conference Call, June 26th, 2002.
[9] Motorola, "Comments on rms AoA spread" 3GPP2 Spatial Channel Modeling Adhoc submission C50-SCM-20020226-002, Feb 26, 2002.
[10] Motorola, "Mobile Angle Spread Measurements and Angle Distribution Model", TSGR1#24(02)0408, Orlando, Florida, USA, February 18-22, 2002.
[11] Texas Instruments, "Parameter Values for the Spatial Channel Model", TSGR1(01)1132, Jeju, Korea, November 19-23, 2001.
[12] Motorola, "A Ray Based MIMO Propagation Model", 3GPP2 TSG-C Submission C50-20010820-027, Portland, OR, August 20-24, 2001
[13] Motorola, "Path Characteristics for Spatial Channel Model", SCM-041, Conference Call, August 1st, 2002.